JACC: CARDIOVASCULAR IMAGING
VOL. 10, NO. 2, 2017

ISSN 1936-878X/$36.00
PUBLISHED BY ELSEVIER
http://dx.doi.org/10.1016/j.jcmg.2016.09.023

Myocardial Blood Flow and Inflammatory Cardiac Sarcoidosis

Matthew J. Kruse, MD,[a] Lara Kovell, MD,[b] Edward K. Kasper, MD,[b] Martin G. Pomper, MD,[a] David R. Moller, MD,[c] Lilja Solnes, MD,[a] Edward S. Chen, MD,[c] Thomas H. Schindler, MD[a,b]

ABSTRACT

OBJECTIVES This study sought to evaluate the effects of inflammatory sarcoid disease on coronary circulatory function and the response to immune-suppressive treatment.

BACKGROUND Although positron emission tomography assessment of myocardial inflammation is increasingly applied to identify active cardiac sarcoidosis, its effect on coronary flow and immune-suppressive treatment remains to be characterized.

METHODS Thirty-two individuals, who were referred for positron emission tomography/computed tomography, were evaluated for known or suspected cardiac sarcoidosis applying ^{18}F-fluorodeoxyglucose to determine inflammation and ^{13}N-ammonia to assess for perfusion deficits following a high-fat/low-carbohydrate diet and fasting state >12 h to suppress myocardial glucose uptake. Inflammation was quantified with standardized uptake value and regional myocardial blood flow at rest and during regadenoson-stimulated hyperemia was determined in ml/g/min. Positron emission tomography studies were repeated in 18 cases with a median follow-up of 2.5 years (interquartile range [IQR]:1.3 to 3.4 years).

RESULTS Twenty-five exams had normal perfusion but evidence of regional inflammation (group 1), and 21 exams presented a regional perfusion deficit associated with inflammation (group 2). Median myocardial blood flow did not differ between inflamed and noninflamed myocardium in both groups (0.86 ml/g/min [IQR: 0.66 to 1.11 ml/g/min] vs. 0.83 ml/g/min [IQR: 0.64 to 1.12 ml/g/min] and 0.74 ml/g/min [IQR: 0.60 to 0.93 ml/g/min] vs. 0.77 ml/g/min [IQR: 0.59 to 0.95 ml/g/min], respectively). As regards median hyperemic myocardial blood flows, they were significantly lower in the inflamed than in the remote regions in group 1 and 2 (2.31 ml/g/min [IQR: 1.81 to 2.95 ml/g/min] vs. 2.70 ml/g/min [IQR: 2.07 to 3.30 ml/g/min] and 1.61 ml/g/min [IQR: 1.17 to 2.18 ml/g/min] vs. 1.94 ml/g/min [IQR: 1.49 to 2.39 ml/g/min]; $p < 0.001$, respectively). Immune-suppression–mediated decrease in inflammation was associated with preserved myocardial flow reserve (MFR) at follow-up, whereas MFR significantly worsened in regions without changes or even increases in inflammation (median ΔMFR: 0.07 [IQR: −0.29 to 0.45] vs. −0.24 [IQR: −0.84 to 0.21]; $p < 0.001$). There was an inverse correlation between pronounced alterations in myocardial inflammation (Δ regional myocardial volume with standardized uptake value >4.1) and ΔMFR ($r = -0.47$; $p = 0.048$).

CONCLUSIONS Sarcoid-mediated myocardial inflammation is associated with a regional impairment of coronary circulatory function. The association between immune-suppressive treatment-related alterations in myocardial inflammation and changes in coronary vasodilator capacity suggests direct adverse effect of inflammation on coronary circulatory function in cardiac sarcoidosis. (J Am Coll Cardiol Img 2017;10:157–67) © 2017 by the American College of Cardiology Foundation.

Sarcoidosis is a multisystem noncaseating granulomatous disease of unclear etiology, resulting from an immune-mediated reaction to a yet unknown antigen in genetically predisposed individuals (1). In the United States, the frequency of cardiac involvement in patients with systemic sarcoidosis is 19% to 25% on autopsy studies, and up to one-half of these patients have clinically

From the [a]Division of Nuclear Medicine-Cardiovascular Section, Department of Radiology and Radiological Science, School of Medicine, Johns Hopkins University, Baltimore, Maryland; [b]Division of Cardiology, Department of Medicine, Johns Hopkins University, Baltimore, Maryland; and the [c]Division of Pulmonary and Critical Care Medicine, Department of Medicine, Johns Hopkins University, Baltimore, Maryland. Supported by Departmental Fund (175470) from Johns Hopkins University. The authors have reported that they have no relationships relevant to the contents of this paper to disclose.

Manuscript received June 1, 2016; revised manuscript received September 12, 2016, accepted September 14, 2016.

ABBREVIATIONS AND ACRONYMS

ANOVA = analysis of variance

CT = computed tomography

CVR = coronary vascular resistance

FDG = ^{18}F-fluorodeoxyglucose

IQR = interquartile range

LV = left ventricular

MBF = myocardial blood flow

MFR = myocardial flow reserve

PET = positron emission tomography

SDS = summed difference score

SUV = standardized uptake value

manifest symptoms (2–4). The most common clinical manifestations are atrioventricular block, ventricular tachycardia, congestive heart failure, and sudden cardiac death (5,6). Clinically, cardiac sarcoidosis is underdiagnosed but it is anticipated to be the predominant cause of death by sarcoidosis in Japan and in the United States (5,6). Within the last decade, a 2-fold increase in sarcoidosis prevalence in the United States has been reported, posing a considerable public health concern (4). The prevalence of sarcoidosis is quite variable and dependent on ethnicity, sex, and regions (6). For example, there is an increased prevalence of sarcoidosis in African Americans as compared to Caucasians with a ratio ranging from 10:1 to 17:1 (6,7). ^{18}F-fluorodeoxyglucose (^{18}F-FDG) positron emission tomography (PET)/computed tomography (CT) in conjunction with ^{13}N-ammonia or ^{82}rubidium PET/CT myocardial perfusion assessment is increasingly applied for the early detection and characterization of inflammatory cardiac sarcoid disease (5), which carries important diagnostic and prognostic information (8). Although ^{18}F-FDG-PET has a reported sensitivity and specificity for the detection of cardiac sarcoid disease as high as 89% and 78%, respectively (9), "physiologic" ^{18}F-FDG uptake may lead to false positive findings despite various strategies for enhanced myocardial suppression of glucose uptake (5). In this respect, it may be intriguing to speculate that alterations in regional myocardial blood flow (MBF) in areas of sarcoid-induced myocardial inflammation may add diagnostic value in avoiding false positive findings. Furthermore, the effect of regional sarcoid disease-related inflammation on hyperemic MBF still remains to be elucidated.

SEE PAGE 168

With this in mind, we aimed to investigate whether sarcoidosis-related inflammation is associated with alterations in resting and hyperemic MBF, and how immune-suppressive treatment would affect inflammation and MBF.

METHODS

STUDY POPULATION. In a retrospective analysis, we investigated 32 consecutive patients referred for an initial cardiac PET/CT examination for the assessment of known or suspected cardiac sarcoidosis January 1, 2009 and June 30, 2015, who had positive myocardial FDG uptake either isolated with normal perfusion or in the region with a perfusion deficit ("mismatch" pattern between abnormal FDG uptake and perfusion deficit) (**Table 1**). Of these 32 patients, 13 underwent 18 repeat examinations with cardiac PET/CT for various indications with a median interval of 1.5 years (interquartile range [IQR]: 0.9 to 3.3 years). The median follow-up was 2.5 years (IQR: 1.3 to 3.4 years) for evaluation of the effect of immune-suppressive medication on cardiac inflammatory disease and MBF. Repeat PET/CT examinations were evaluated and compared with baseline PET/CT examinations. In all patients, cardiovascular risk factors and the clinical presentations, such as heart block, ventricular arrhythmia, or heart failure, were recorded. Previous cardiac biopsy positive for sarcoid, previous PET or cardiac magnetic resonance compatible with cardiac sarcoidosis, prednisone dose at time of imaging, and other immunosuppressive medication use was documented. All vasoactive medications such as calcium channel blockers, angiotensin-converting enzyme inhibitors, long-acting nitrates, or beta adrenergic blockers were withheld for at least 48 h prior to the PET studies. The study was approved by the Johns Hopkins Institutional Review Board (No. 00063412) and conducted in agreement with institutional guidelines.

PET/CT ASSESSMENT OF MYOCARDIAL PERFUSION. ^{13}N-ammonia PET determined myocardial perfusion and MBF in ml/min/g with serial image acquisition (64-slice Discovery Rx VCT PET/CT [GE Healthcare, Milwaukee, Wisconsin]) and a 2-compartment tracer kinetic model in a single rest-stress protocol. Following the topogram used to define the axial field-of-view and a low-dose CT scan (120 kV, 30 mA) for attenuation correction, PET emission data were acquired in fully 3-dimensional mode during shallow breathing following intravenous injection of ^{13}N-ammonia. At first, PET scanning at rest started immediately following injection of ≈10 mCi of ^{13}N-ammonia for a total duration of 20 min in list-mode format and 36 dynamic frames were reconstructed using iterative normalized attenuation-weighted ordered subsets expectation maximization. The CT-based attenuation correction map was used to reconstruct the PET emission data. An interval of ≈45 to 60 min was allowed for radiotracer decay of ^{13}N-ammonia from the first injection, before starting the subsequent stress protocol. PET image acquisition during regadenoson-stimulated hyperemia (0.4 mg intravenous bolus injection over 10- and 20-s intervals) was started immediately following injection of ≈10 mCi of ^{13}N-ammonia again for a total duration of 20-min list-mode PET data

TABLE 1 Clinical Characteristics of the Study Population

Age, yrs	49.5 (48.0-55.5)
Male/female	17 (53)/15 (47)
Cardiac risk factors	
Hypertension	14 (44)
Hyperlipidemia	13 (41)
Diabetes mellitus	1 (3)
Ever smoked	8 (25)
Family history of cardiac disease	7 (22)
BMI >30 kg/m^2	18 (56)
Primary cardiac symptoms	
Advanced atrioventricular block	16 (50)
Ventricular arrhythmia	12 (38)
Heart failure/cardiomyopathy	3 (9)
Sinus arrhythmia	1 (3)
Clinical/diagnostic parameters positive for cardiac sarcoidosis	
2006 JMHW criteria*	19 (59)
Modified JMHW criteria*	30 (94)
Negative cardiac catheterization	11 (34)
Sarcoid biopsy (any systemic site)	26 (81)
Cardiac sarcoid biopsy	3 (9)
Prior sarcoid-protocol PET	3 (9)
DE CMR	18 (56)
Treatment	
No prednisone	15 (47)
Treated with prednisone	17 (53)†
Other immunosuppressive medication	9 (28)‡
Beta blocker	21 (66)
ACE-I/ARB	9 (28)
Antiarrhythmic	5 (16)
Aldosterone inhibitor	3 (9)

Values are median (IQR) or n (%). *The 2006 JMHW criteria are the original criteria for diagnosis of cardiac sarcoidosis; modified JHMW criteria are the adapted criteria in McArdle et al. (16). †Median daily dose 20 mg (IQR: 10 to 20 mg). ‡Mycophenolate mofetil (5 patients), methotrexate (n = 3), azathioprine (n = 1).

ACE-I = angiotensin-converting enzyme inhibitor; ARB = angiotensin II receptor blocker; BMI = body mass index; DE CMR = delayed enhancement cardiac magnetic resonance; IQR = interquartile range; JMHW = Japanese Ministry of Health and Welfare; PET = positron emission tomography.

acquisition. The stress and rest PET images were visually checked for accurate alignment with the CT scan used for attenuation correction. In case of misalignment between PET and CT images, CT data were shifted in the horizontal and anterior-posterior directions in the transaxial planes and in the superior-inferior direction of coronal planes, to visually align the heart borders visible on CT with the PET emission data and achieve an accurate coregistration (10). Static 20-min myocardial perfusion images at rest and during regadenoson-induced hyperemia were evaluated visually on reoriented short- and long-axis myocardial slices and semiquantitatively on the corresponding polar map displays. For the semiquantitative analysis of the PET perfusion images, a 17-segment model and a 5-point grading system by 2 expert observers were used (11). Summed stress score, summed rest score, and summed difference score (SDS) were determined. A summed stress score <4 was considered normal, 4 to 8 mildly abnormal, 9 to 13 moderately abnormal, and >13 severely abnormal perfusion defect. In addition, a SDS ≥2 signified a reversible perfusion defect, whereas <2 was deemed normal. The extent of regional reversible perfusion defects on ^{13}N-ammonia PET/CT images was scored according to the SDS value. For MBF quantification, left ventricular (LV) contours and input function region were obtained automatically with minimal operator intervention in QPET software (Cedars-Sinai, Los Angeles, California) as described previously (12). The rest and hyperemic MBF were quantified within the whole LV region bounded by the LV plane. In addition, the myocardial flow reserve (MFR) was computed by dividing each stress polar map sample by the rest samples at each point. Regional MBF in ml/g/min of the myocardial regions supplied by the left anterior descending, left circumflex, and right coronary arteries were averaged on a polar map and defined as mean MBF of the LV. Segmental MBF of the LV myocardium was evaluated on a 17-segment model. To compensate for interindividual variations in coronary driving pressure during hyperemic flows, an index of coronary vascular resistance (CVR) was determined as the ratio of mean arterial blood pressure (mm Hg) to MBF (ml/g/min). Finally, electrocardiography-gated list-mode data were reconstructed to 8 gated frames and processed with QPET, using automatic contouring of the LV at each frame and manual adjustment as needed. Based on the contours, the end-diastolic volume, the end-systolic volume, and corresponding LV ejection fraction) were calculated.

FDG-PET/CT MEASUREMENT OF INFLAMMATION. Following myocardial perfusion imaging, patients underwent metabolic imaging using ^{18}F-FDG with a whole-body and dedicated cardiac PET/CT scan. Prior to the ^{18}F-FDG PET/CT examination, the patient had a very high-fat, low-carbohydrate, protein-permitted diet the day before followed by a 12-h fasting state to sufficiently suppress physiologic glucose and thus ^{18}F-FDG myocardial uptake (13,14). Patients were also instructed to avoid any exercise for at least 48 h. Images were evaluated independently by 2 experienced readers. In cases of disagreement between the 2 readers, consent was achieved in a joint reading. Approximately 60 min after intravenous injection of 0.135 mCi/kg ^{18}F-FDG, a whole-body PET scan from the base of the skull to mid thighs was acquired. Following whole-body imaging (5 to 7 bed positions with 4-min acquisition), dedicated cardiac

PET scan over 20 min was performed. Images were reconstructed by normalized attenuation-weighted ordered subsets expectation maximization with attenuation correction and displayed along the perfusion images in short, vertical long, and horizontal long axes (8). Perfusion- and FDG-PET/CT images were grouped into the following patterns: normal perfusion and metabolism, abnormal perfusion or metabolism, or abnormal perfusion and metabolism (8). Normal metabolism was defined as complete suppression of FDG from the myocardium. Patients with diffuse FDG uptake without any areas of focal uptake were excluded from the study as the findings may have reflected unsuccessful suppression of myocardial glucose uptake and/or noncompliant patients to dietary restrictions and fasting sarcoid preparation protocol. Segmental metabolic evaluation was performed using similar semiautomated processing of FDG-PET/CT images with QPET. Using visual analysis, involvement of individual segments with abnormal FDG activity (classified as >50% of the segment area demonstrating abnormal activity) was assessed. Maximum standardized uptake value (SUV) and metabolic volume above previously published SUV thresholds (regional myocardial volume with SUV >2.7 and SUV >4.1) was calculated using Mirada XD3 software (Mirada Medical, Twin Falls, Idaho) (15). SUV measurements were calculated both according to body weight and lean body mass. Responders to immune-suppressive medication were defined by a decrease of maximum cardiac SUV normalized to mean liver uptake. Whole-body FDG images were evaluated by physicians who were blinded to the cardiac PET/CT results to determine any active extracardiac disease.

STATISTICS. Because continuous variables are not always normally distributed, they are presented as median (IQR) (i.e., 25th to 75th percentile; Q1, Q3). For comparison of differences, Mann-Whitney *U* test for independent samples was used (SPSS Statistics version 23, IBM, Armonk, New York). When analyzing differences between baseline and repeat PET/CT measurements, Wilcoxon test for related samples was used. A comparison of differences in MBF and FDG uptake among regions between groups 1 and 2 was performed by 1-way analysis of variance (ANOVA), followed by Scheffé multiple comparison test. No corrections were applied to segment-wise analyses for multiple observations within individuals. Spearman rank-order correlation coefficient (r), assuming a linear regression, was calculated to investigate the associations between regional MBF and FDG uptake. Statistical significance was assumed if the null hypothesis could be rejected at $p < 0.05$.

RESULTS

CLINICAL CHARACTERISTICS. Table 1 summarizes the clinical characteristics and primary cardiac symptoms of the study population. Of the 32 patients, 19 (59%) met the Japanese Ministry of Health and Welfare 2006 criteria for diagnosis of cardiac sarcoid, and 30 (94%) met the modified Japanese Ministry of Health and Welfare criteria published more recently (16). The baseline PET results demonstrated normal perfusion but abnormal FDG uptake in 18 patients (56%) and regional perfusion deficit with abnormal FDG uptake (mismatch pattern) in 14 patients (44%).

BASELINE FINDINGS OF PET/CT. In patients with normal perfusion but abnormal FDG uptake (group 1), the intrapatient comparison between FDG positive (+) and FDG negative (-) regions demonstrated similar resting MBF (Figure 1, Table 2). Regional MBF during hyperemic flow stimulation with regadenoson was significantly lower in FDG (+) than in FDG (-) territories (Figure 1). Similarly, the regional MFR was significantly lower in FDG (+) than in FDG (-) territory. To further substantiate these observations, the corresponding regional CVR was also evaluated and related to the FDG uptake findings. Indeed CVR during hyperemic flow stimulation was significantly higher in FDG (+) than in FDG (-) territory. In group 1, therefore, hyperemic MBF and MFR were impaired in the inflamed region compared with the noninflamed region (Figure 1).

In group 2, defined by abnormal FDG uptake in the area of the perfusion deficit (mismatch pattern), the intrapatient comparison between FDG (+) and FDG (-) regions also demonstrated comparable resting MBF (Figure 1, Table 2). Resting MBF in FDG (+) and FDG (-) regions in group 2 were significantly lower compared with the corresponding regions in group 1 ($p = 0.004$ and $p = 0.009$, respectively). Regional hyperemic MBF and MFR, however, were significantly reduced in FDG (+) than in FDG (-) territories (Figure 1, Table 2). The evaluation of CVR during hyperemic flow stimulation also widely mirrored the hyperemic MBF values, emphasizing an impairment of hyperemic MBF increases in regions with abnormal FDG uptake. Interestingly, hyperemic MBF in group 2 in FDG (+) and (-) regions were also significantly less than corresponding regions in group 1 (both $p < 0.001$). The resting MBF among regions differed significantly between groups 1 and 2

FIGURE 1 Regional MBF and Inflammation

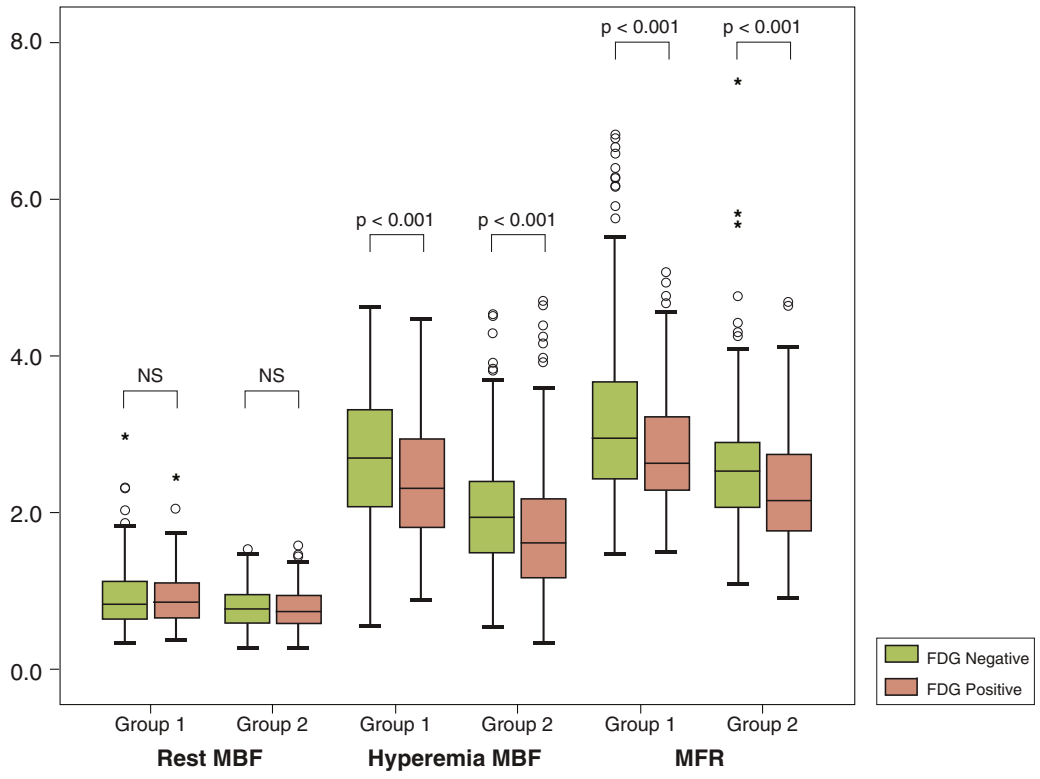

Myocardial blood flow (MBF) at rest, during hyperemic flow stimulation, and corresponding myocardial flow reserve (MFR) in group 1 and group 2 in fluorodeoxyglucose (FDG) **– (green bars)** and **+ (pink bars)** myocardial regions. Box plot display with median, interquartile range **(box),** minimum and maximum **(2-sided bar)**, outliers **(circles)** and extreme outliers **(asterisks)**.

($p \leq 0.001$ by ANOVA). Also, regadenoson-induced hyperemic MBF, MFR, and CVR during hyperemia, among regions was significantly different between both groups ($p \leq 0.001$ by ANOVA, respectively). Hyperemic MBF and MFR were significantly greater in group 1 than in group 2, for both FDG (+) and FDG (-) regions ($p < 0.001$). Finally, as regards regional myocardial inflammation in the whole study group at baseline, regional myocardial maximum SUV and metabolic volumes did not correlate with hyperemic MBF, CVR during hyperemia, and MFR, respectively (Table 3).

TABLE 2 Myocardial Flow Parameters and FDG Findings in the Study Population

	Group 1: Normal Perfusion and FDG (+) Findings (n = 25)			Group 2: Regional Perfusion Deficit With FDG (+) Findings ("Mismatch") (n = 21)		
	FDG (+) Segments (n = 135)	FDG (-) Segments (n = 290)	p Value	FDG (+) Segments (n = 138)	FDG (-) Segments (n = 219)	p Value
Rest MBF, ml/g/min	0.86 (0.66-1.11)	0.83 (0.64-1.12)	0.559	0.74 (0.60-0.93)	0.77 (0.59-0.95)	0.494
Hyperemic MBF, ml/g/min	2.31 (1.81-2.95)	2.70 (2.07-3.30)	<0.001	1.61 (1.17-2.18)	1.94 (1.49-2.39)	<0.001
MFR	2.63 (2.27-3.24)	2.95 (2.45-3.70)	<0.001	2.16 (1.78-2.73)	2.53 (2.07-2.90)	<0.001
CVR at rest, mm Hg/ml/g/min	109.5 (83.1-142.9)	111.3 (82.3-140.6)	0.753	122.5 (93.3-149.7)	111.4 (90.2-145.7)	0.264
CVR during hyperemia, mm Hg/ml/g/min	41.0 (31.3-52.7)	33.2 (26.7-45.0)	<0.001	53.7 (38.8-74.3)	43.9 (35.4-57.8)	<0.001

Values are median (IQR). Paired analysis between FDG positive (+) and FDG negative (-) myocardial regions.

CVR = coronary vascular resistance; FDG = ^{18}F-fluorodeoxyglucose; IQR = interquartile range; MBF = myocardial blood flow; MFR = myocardial flow reserve.

TABLE 3 Correlations Among Myocardial Flow Parameters and Myocardial Inflammation at Baseline Study

	Regional Myocardial Maximum SUV	Regional Myocardial Volume With SUV >2.7	Regional Myocardial Volume With SUV >4.1
Rest MBF, ml/g/min	r = -0.005 p = 0.977	r = 0.001 p = 0.999	r = -0.007 p = 0.970
Hyperemic MBF, ml/g/min	r = -0.066 p = 0.720	r = -0.128 p = 0.486	r = -0.087 p = 0.634
MFR	r = -0.145 p = 0.429	r = -0.194 p = 0.288	r = -0.176 p = 0.335
CVR at rest, mm Hg/ml/g/min	r = 0.158 p = 0.388	r = 0.138 p = 0.452	r = 0.132 p = 0.472
CVR during hyperemia, mm Hg/ml/g/min	r = 0.171 p = 0.348	r = 0.246 p = 0.175	r = 0.220 p = 0.226

r = Spearman's rank-order correlation coefficient; SUV = standardized uptake value (g/ml); other abbreviations as in Table 2.

LONGITUDINAL FOLLOW-UP STUDY. Patients were followed up with cardiac PET examination most commonly for evaluation of treatment response after 6 months or for prednisone titration within 6 months. Other reasons for follow-up assessment were recurrent ventricular tachycardia, implantable cardioverter-defibrillator firing, weight gain, heart block, and heart failure worsening (Table 4). Among all patients, there was a nonsignificant paradoxical increase in regional myocardial maximum SUV and volumes greater than SUV thresholds at follow-up when compared with baseline values (Table 4). However when subgrouping the follow-up study population into groups of responders (n = 8) and nonresponders (n = 10) to immune-suppressive treatment (Table 5), the regional myocardial maximum SUV and metabolic volumes significantly decreased and increased, respectively. As a consequence, the change (from baseline to follow-up) in regional myocardial maximum SUV and metabolic volumes showed significant worsening in the nonresponder group compared with the responder group (Figures 2A and 2B, Table 6). Responders to immune-suppressive medication had a higher median daily prednisone dose of 20 mg (IQR: 9.4 to 32.5 mg) as compared with nonresponders with 13 mg (IQR: 7.5 to 20.0 mg). This difference, however, did not achieve statistical significance (p = 0.328). Steroid-sparing medication with mycophenolate (2 g/day) was added in 4 cases in both groups. In nonresponders, azathioprine (2 mg/kg/day), leflunomide (20 mg/day), and methotrexate (7.5 mg/week) were each added once (Table 5).

With respect to hemodynamics, the heart rate, systolic blood pressure, and rate-pressure product at rest did not differ significantly between baseline and follow-up examination (Table 4). Resting global MBF on repeat assessment was mildly but nonsignificantly lower at follow-up, respectively (Table 4). Regadenoson-stimulated global MBF was lower at follow-up than at baseline (p = 0.034). The global MFR and CVR during regadenoson stimulation did not differ significantly. In group 2, the median initial SRS, summed stress score, and SDS were 7 (IQR: 1 to 11), 11 (IQR: 5 to 16), and 2 (IQR: 1 to 4) respectively. This did not alter significantly at follow-up with medians of 10 (IQR: 6 to 13), 12 (IQR: 7 to 17), and 3 (IQR: 2 to 4), respectively. When regarding groups of responders and nonresponders according to immune-suppression induced decreases in inflammation, the global and regional resting MBF were lower at follow-up than at baseline in both responders and non-responders (Table 5). However the change in global resting MBF (ΔMBF rest = rest MBF at follow-up – rest MBF at baseline) showed a larger decrease in responders than in nonresponders (Table 6). As regards global and regional hyperemic MBF, they decreased significantly in both groups of responders and nonresponders (Table 5). The change in global hyperemic MBF (Δ hyperemic MBF = hyperemic MBF at follow-up - hyperemic MBF at baseline) was not significantly more pronounced in nonresponders than in responders; however, the CVR during regadenoson (ΔCVR during hyperemia) increased more in nonreponders (p = 0.020) (Table 6). In addition, the change in global MFR (ΔMFR = MFR at follow-up - MFR at baseline) demonstrated a greater decrease in nonresponders than responders (Figure 2C). The group comparison of the global ΔCVR during hyperemia and ΔMFR was statistically significant among both responders and nonresponders (p = 0.001 by ANOVA). Coronary circulatory function in the group of nonresponders, therefore, worsened significantly when compared with the group of responders. The relationship between changes in SUV and coronary circulatory function in patients during follow-up was also evaluated. As can be appreciated in Table 7, there were no correlations between changes in regional myocardial maximum SUV and Δhyperemic MBF or ΔCVR during hyperemia. However there was a significant inverse correlation between Δregional myocardial volume with SUV >4.1 and ΔMFR (r = -0.47; p = 0.048) and borderline significant correlation between Δregional myocardial volume with SUV >2.7 and ΔMFR (r = -0.44; p = 0.066) (Figures 3A and 3B). Finally, the relationship among alterations in LV ejection fraction, end-diastolic volume, end-systolic volume, and coronary circulatory function during follow-up was assessed. There were no significant associations among changes in

hyperemic MBF or MFR with alterations in LV ejection fraction and end-diastolic volume during follow-up ($r = 0.168$, $p = 0.505$; $r = -0.389$, $p = 0.111$ and $r = 0.131$, $p = 0.605$; $r = -0.434$, $p = 0.072$), whereas both ΔHyperemic MBF and ΔMFR correlated significantly and inversely with alterations in end-systolic volume ($r = -0.515$, $p = 0.029$ and $r = -0.609$, $p = 0.007$).

DISCUSSION

The observation of the current study provides several novel observations. First, sarcoid-induced myocardial inflammation per se did not affect resting MBF. Such findings may outline that regional myocardial inflammation does not overcome the active autoregulation of coronary flow in dependency of myocardial metabolic demand (17). Second, hyperemic MBF and MFR were significantly lower in the inflamed as compared to the noninflamed myocardial region, suggesting an adverse effect of sarcoid-related myocardial inflammation on regional coronary circulatory function. Third, immune-suppressive treatment mediated decreases in myocardial inflammation were associated with maintained coronary circulatory function at follow-up. Conversely, ineffective immune suppression with unchanged or even increased myocardial inflammation resulted in a marked worsening of coronary circulatory function during the follow-up period. Fourth, the observed significant association between decreased myocardial inflammation and alterations in MFR emphasizes a direct adverse effect of sarcoid-related myocardial inflammation on coronary vasodilator capacity. These findings may outline an adverse effect of sarcoidosis-induced myocardial inflammation on coronary circulatory function, potentially defining a mechanistic link between inflammatory sarcoid activity and increased cardiovascular risk as recently reported (8).

INFLAMMATION AND HYPEREMIC MBF. Regional hyperemic MBF and MFR were significantly lower in the inflamed than in the noninflamed remote myocardial regions. Sarcoid-induced myocardial inflammation, therefore, was accompanied by abnormal function of the coronary circulation. Of interest and somewhat surprising, there was a dissociation between the extent of myocardial inflammation and hyperemic flow parameters at baseline measurements. The reason for this remains uncertain, but may be related to preventive medical care of coexisting cardiovascular risk factors (such as arterial hypertension, type 2 diabetes mellitus, or heart failure) resulting in favorable effect on coronary circulatory dysfunction (18,19). In addition, coronary circulatory function may deteriorate before sarcoid-induced structural alterations of the myocardium manifest, which may have also contributed to this lack of association. The observed heterogeneity in coronary circulatory function of the LV may also reflect a pathophysiological

TABLE 4 Findings of Baseline and Follow-Up Studies in Sarcoid Patients

	Baseline	Follow-Up	p Value
Age, yrs	46 (40.5–55.5)		
Male/female	8/5		
BMI, kg/m^2	33.6 (30.1–40.2)	38.5 (32.9–39.6)	0.514
Risk factors			
Hypertension	62 (8)	61 (11)	0.981
Hyperlipidemia	54 (7)	56 (10)	0.925
Diabetes	0 (0)	0 (0)	–
Tobacco use	18 (2)	22 (4)	0.999
Familial history of CAD	18 (2)	17 (3)	0.999
Obesity	77 (10)	89 (16)	0.625
Reason for follow-up scan			
Treatment response after 6 months		33 (6)	–
Prednisone titration (<6 months)		22 (4)	–
Recurrent VT/ICD firing		22 (4)	–
Weight gain/fatigue*		11 (2)	–
Heart block		6 (1)	–
Heart failure worsening		6 (1)	–
Hemodynamics			
Rest HR, beats/min	73 (69–77)	70 (65–78)	0.441
Hyperemia HR, beats/min	91 (85–112)	88 (82–94)	0.183
Rest SBP, mm Hg	135 (120–144)	123 (117–136)	0.258
Hyperemia SBP, mm Hg	142 (113–154)	131 (113–142)	0.441
Rest MAP, mm Hg	93 (82–98)	84 (81–89)	0.157
Hyperemia MAP, mm Hg	93 (77–99)	85 (77–90)	0.275
Rest RPP	9,180 (8,037–11,011)	8,763 (7,824–9,497)	0.312
Hyperemia RPP	12,768 (10,524–15,177)	10,995 (9903–12,427)	0.089
Global MBF			
Rest MBF, ml/g/min	0.82 (0.69–1.06)	0.73 (0.62–0.91)	0.183
Hyperemic MBF, ml/g/min	2.36 (1.72–2.94)	1.74 (1.49–2.33)	0.034
MFR	2.75 (2.23–3.18)	2.27 (1.99–3.01)	0.135
CVR at rest, mm Hg/ml/g/min	100 (90–132)	114 (95–135)	0.489
CVR during hyperemia, mm Hg/ml/g/min	40 (30–49)	47 (38–53)	0.258
Regional metabolic assessment			
Myocardial Maximum SUV, g/ml	4.2 (0–5.8)	5.3 (2.3–8.2)	0.622
Myocardial Volume with SUV >2.7, g/ml	22.2 (0–140.0)	22.3 (0–164.2)	0.984
Myocardial Volume with SUV >4.1, g/ml	0 (0–2.8)	3.4 (0–54.3)	0.417
Function and volumes of LV			
LVEF, %	44 (33–52)	46 (42–57)	0.933
EDV, ml	128 (103–199)	135 (103–200)	0.176
ESV, ml	76 (45–133)	69 (39–137)	0.185

Values are median (IQR) or % (n). *Steroid side effects and desire of the patient to decrease steroid dose.

CAD = coronary artery disease; EDV = end-diastolic volume; ESV = end-systolic volume; HR = heart rate; ICD = implantable cardioverter-defibrillator; LVEF = left ventricular ejection fraction; MAP = mean arterial pressure; RPP = rate-pressure product; SBP = systolic blood pressure; VT = ventricular tachycardia; other abbreviations as in Tables 1 and 2.

TABLE 5 Myocardial Flow, LVEF, FDG Findings, and Immune-Suppression of the Follow-Up Study in Treatment Responders and Nonresponders

	Responders			Nonresponders		
	Baseline	Follow-Up	p Value	Baseline	Follow-Up	p Value
Global rest MBF, ml/g/min	0.96 (0.75–1.12)	0.78 (0.64–0.96)	<0.001	0.70 (0.59–0.91)	0.67 (0.52–0.92)	0.030
Regional rest MBF, ml/g/min	0.93 (0.80–1.18)	0.75 (0.59–0.95)	<0.001	0.78 (0.61–0.93)	0.69 (0.52–0.98)	0.253
Global hyperemic MBF, ml/g/min	2.26 (1.67–2.99)	1.91 (1.50–2.44)	<0.001	2.07 (1.45–2.96)	1.71 (1.24–2.18)	<0.001
Regional hyperemic MBF, ml/g/min	2.60 (1.67–3.11)	1.96 (1.57–2.29)	<0.001	1.88 (1.27–2.26)	1.69 (1.19–2.06)	0.010
Global MFR	2.41 (1.93–3.00)	2.50 (1.94–3.05)	0.272	2.64 (2.02–3.51)	2.25 (1.82–2.83)	<0.001
Regional MFR	2.48 (2.15–3.11)	2.63 (2.12–3.05)	0.922	2.42 (1.78–2.95)	2.12 (1.79–2.45)	0.032
Global CVR at rest, mm Hg/ml/g/min	96 (81–120)	107 (86–135)	<0.001	121 (95–149)	129 (95–160)	0.127
Regional CVR at rest, mm Hg/ml/g/min	96 (83–120)	118 (90–156)	<0.001	119 (96–140)	124 (85–165)	0.322
Global CVR – hyperemia, mm Hg/ml/g/min	39 (30–51)	42 (33–53)	0.009	43 (30–60)	51 (40–70)	<0.001
Regional CVR- hyperemia, mm Hg/ml/g/min	35 (29–49)	48 (36–56)	0.012	47 (36–63)	51 (41–73)	0.187
Regional myocardial maximum SUV, g/ml	4.2 (2.1–5.7)	2.3 (1.7–2.6)	0.009	4.0 (2.5–6.3)	6.9 (5.5–13.0)	0.005
Regional myocardial volume with SUV >2.7, g/ml	29.3 (0–114.8)	0 (0–0)	0.050	9.2 (0–147.7)	132.4 (26.8–392)	0.011
Regional myocardial volume with SUV >4.1, g/ml	0 (0–17.7)	0 (0–0)	0.043	0.1 (0–29.1)	27.8 (4.8–208.6)	0.011
Rest LVEF, %	47 (41–56)	52 (44–59)	0.441	45 (33–56)	44 (39–50)	0.683
Rest EDV, ml	105 (84–132)	126 (86–142)	0.674	159 (75–227)	165 (100–279)	0.139
Rest ESV, ml	55 (32–79)	52 (35–80)	0.673	95 (32–142)	101 (48–156)	0.059
Immune-suppressive treatment						
Prednisone		75 (6)			90 (9)	
Nonsteroids		50 (4)			70 (7)	
None		13 (1)				

Values are median (IQR) or % (n). p Values versus baseline in each group (Wilcoxon signed ranks test). Regional MBF reflects the area with FDG positive (+) segments at baseline.
Abbreviations as in Tables 1 to 4.

substrate underlying the development of arrhythmia such as ventricular tachycardia or ventricular fibrillations, observed in 38% of the current study population.

When comparing group 1 (inflammation only) and group 2 (inflammation and perfusion deficit), patients in group 1 demonstrated a more pronounced hyperemic flow difference between inflamed and

FIGURE 2 Alterations in Myocardial Inflammation and Coronary Vasodilator Capacity After Treatment Follow-Up

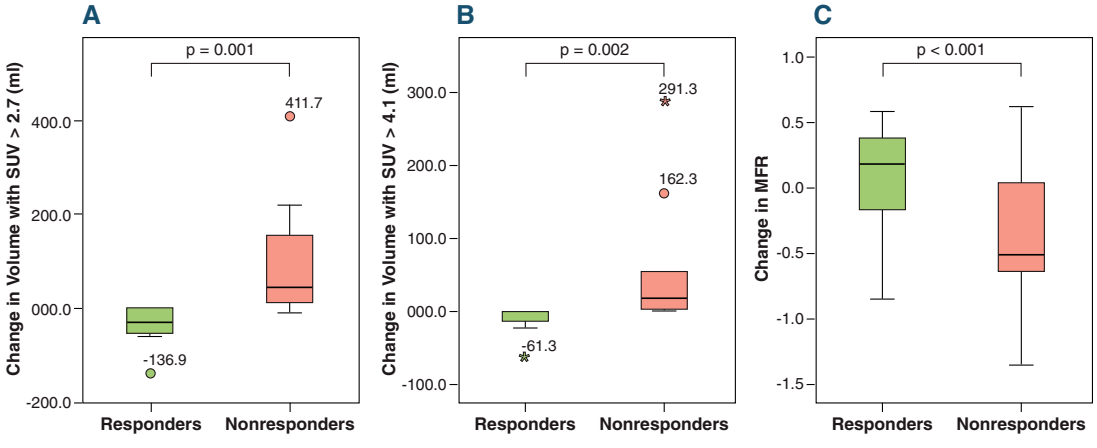

(A) Change in myocardial inflammation (volume with standardized uptake value [SUV] >2.7) after treatment period in responders **(green bar)** and nonresponders **(pink bar). (B)** Change in myocardial inflammation (volume with SUV >4.1) after treatment period in responders **(green bar)** and nonresponders **(pink bar). (C)** Corresponding alteration in myocardial flow reserve (MFR) in treatment responders **(green bar)** and nonresponders **(pink bar)**. Box plot display with median, interquartile range **(box)**, minimum and maximum **(2-sided bar)**, outliers **(circles)** and extreme outliers **(asterisks)**.

remote myocardium regions. Patients in group 1 also had a significantly shorter median time from symptom onset until PET/CT than did those in group 2 (1.17 years [IQR: 0.67 to 4.08] vs. 2.75 years [IQR: 1.83 to 6.00]). These observations suggest that in the early stage of inflammation, alterations in coronary circulatory function are largely confined to the inflamed regions and have not yet affected the remote myocardium. Conversely, in more advanced stages of cardiac sarcoidosis (represented by group 2), dysfunction of the coronary circulation does not appear to be limited to the inflamed regions but rather also involves remote regions but less in severity. Such observations may suggest development of diffuse impairment of coronary circulation in cardiac sarcoidosis, which could precede the negative remodeling and/or structural alterations such as interstitial fibrosis (20) that over time can advance into sarcoidosis-induced heart failure. However, this theory requires further investigation.

INFLAMMATION AND RESTING MBF. Resting MBF did not differ significantly between inflamed and remote myocardium in both groups. It is possible that although the relative regional reduction in myocardial perfusion is commonly related to sarcoid-induced myocardial fibrosis and/or even necrosis, it can also reflect myocardial edema in the acute inflammatory setting with only mildly altered MBF (5,6). In addition, mild heterogeneities in resting myocardial perfusion may not be associated with marked differences in resting MBF and within the variability of individual resting MBF ranging from 0.4 to 1.2 ml/g/min (17,19). Thus, the evaluation of regional resting MBF may not add further information in characterizing regional inflammation or in identifying false positive findings on myocardial FDG images.

EFFECTS OF STEROID MEDICATION. After a median follow-up of 2.5 years, steroid treatment had effectively reduced myocardial inflammation in 8 follow-up cases, but insufficiently in the other 10 follow-up cases. In treatment responders as defined by markedly reduced regional myocardial inflammation, coronary circulatory dysfunction widely remained preserved. Conversely, hyperemic flow response and MFR had further significantly declined in nonresponders after the follow-up period. The reason for the inadequate treatment response in nonresponders is uncertain. It may be related to a relatively short duration of 6 months' standard steroid treatment approach, early tapering of steroid dose with suboptimal treatment timing, the use of potentially less effective other nonsteroid immune suppression, and unknown period of remission after treatment response in inflammatory cardiac sarcoidosis. In addition, yet unknown metabolic/genetic factors or suboptimal patient compliance may also have accounted for observed insufficient treatment response in a subset of patients (5,15).

The observed association between decrease in myocardial inflammation and preserved coronary circulatory function indicates that effects of immune-suppressive medication had directly prevented a further deterioration of the coronary vasodilator capacity. Possible mechanisms underlying the beneficial effects of the immune-suppressive medication on sarcoid-related

TABLE 6 Change in Myocardial Flow Parameters and FDG Findings Between Baseline and Follow-Up Study in Treatment Responders and Nonresponders

	Responders	Nonresponders	p Value
ΔRest MBF, ml/g/min	-0.11 (-0.29 to -0.02)	-0.05 (-0.17 to 0.09)	<0.001
ΔHyperemic MBF, ml/g/min	-0.26 (-0.82 to 0.09)	-0.22 (-0.71 to 0.04)	0.915
ΔMFR	0.07 (-0.29 to 0.45)	-0.24 (-0.84 to 0.21)	<0.001
ΔCVR at rest, mm Hg/ml/g/min	8.7 (-3.9 to 23.2)	5.4 (-22.5 to 31.1)	0.130
ΔCVR during hyperemia, mm Hg/ml/g/min	4.1 (-8.3 to 14.0)	5.6 (-2.6 to 21.5)	0.020
ΔRegional myocardial maximum SUV, g/ml	-1.9 (-3.7 to -0.1)	3.5 (2.2 to 4.9)	<0.001
ΔRegional myocardial volume with SUV >2.7, g/ml	-29.3 (-55.8 to 0)	48.0 (9.9 to 171.0)	0.001
ΔRegional myocardial volume with SUV >4.1, g/ml	0 (-17.7 to 0)	15.0 (0.3 to 80.2)	0.002

Values are median (IQR).
Abbreviations as in Tables 1 to 4.

TABLE 7 Correlations Among Changes in Myocardial Flow Parameters and Myocardial Inflammation Between Baseline and Follow-Up Studies

	Δ Regional Myocardial Maximum SUV (g/ml)	Δ Regional Myocardial Volume With SUV > 2.7 (g/ml)	Δ Regional Myocardial Volume With SUV > 4.1 (g/ml)
ΔRest MBF, ml/g/min	r = 0.315 p = 0.203	r = 0.392 p = 0.108	r = 0.441 p = 0.067
ΔHyperemic MBF, ml/g/min	r = 0.194 p = 0.440	r = -0.021 p = 0.933	r = -0.027 p = 0.916
ΔMFR	r = -0.204 p = 0.418	r = -0.442 p = 0.066	r = -0.472 p = 0.048
ΔCVR at rest, mm Hg/ml/g/min	r = -0.379 p = 0.121	r = -0.442 p = 0.066	r = -0.549 p = 0.018
ΔCVR during hyperemia, mm Hg/ml/g/min	r = -0.176 p = 0.484	r = -0.080 p = 0.753	r = -0.088 p = 0.728

Abbreviations as in Tables 1 to 4.

FIGURE 3 Association Among Treatment-Related Alterations in Myocardial Inflammation and Coronary Vasodilator Capacity

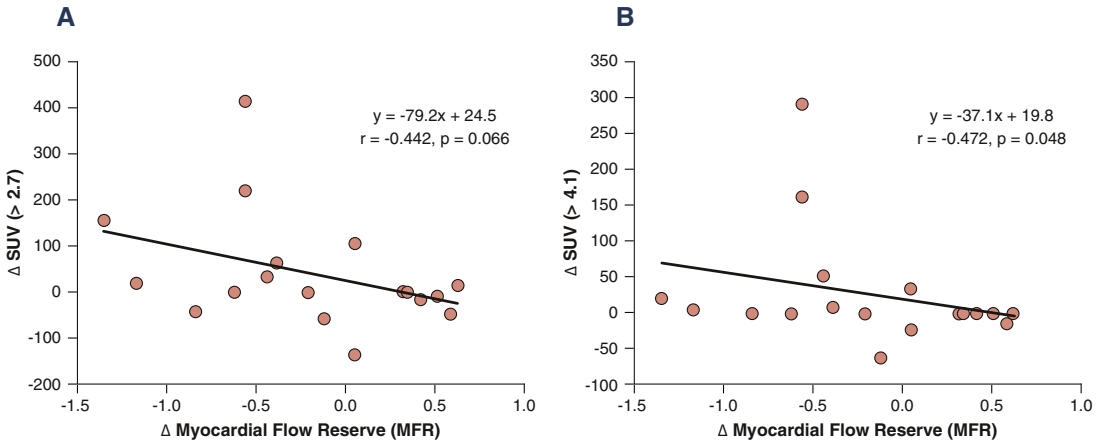

Correlation of alterations in inflammation and MFR with different thresholds of SUV such as change in volume >2.7 **(A)** and >4.1 **(B)**. Abbreviations as in Figure 2.

vasculopathy include reduction in myocardial inflammation, reduced proliferation of vascular smooth muscle cells and fibrous tissue, decreased oxidative stress burden in the arterial wall, and as yet unknown factors (5,6). Of note, a dysregulation of the communication between coronary endothelial cells and cardiomyocytes has been suggested to play a central role in the development of cardiac structural and functional abnormalities leading to heart failure (20) that warrants further investigation in cardiac sarcoidosis.

STUDY LIMITATIONS. First, in the current study population, we cannot exclude entirely that the use of vasodilators for stress perfusion imaging did not have some minor metabolic effects on subsequent FDG uptake. However, the study conditions were exactly the same between baseline and repeat PET examination, and no additional or enhanced regional perfusion deficits during vasomotor stress were noted. Thus potential confounding effects of regional ischemia during pharmacologic vasodilation on observed FDG uptake are unlikely to have occurred. Second, an unanticipated observation was the weak but significant inverse association between alterations in coronary circulatory function and end-systolic volume. Although the reasons for this correlation remain uncertain, it may be related to alterations in hyperemic coronary flow associated with changes in oxygen consumption and contractile function, the so-called Gregg phenomenon (17). Third, the sample size of the study population is relatively small. Current findings do not allow generalized conclusions, but they might hopefully stimulate further large-scale clinical trials in the imaging of cardiac sarcoidosis activity and response to immune-suppressive therapy.

CONCLUSIONS

Sarcoid-mediated myocardial inflammation is associated with a regional impairment of coronary circulatory function. The close association between steroid treatment-related alterations in myocardial inflammation and changes in coronary vasodilator capacity suggests direct adverse effect of inflammation on coronary circulatory function in cardiac sarcoidosis.

ACKNOWLEDGMENTS The authors thank Corina Voicu and Jeannie Peters for assisting in the PET studies, and the cyclotron staff for ^{13}N-ammonia production.

ADDRESS FOR CORRESPONDENCE: Dr. Thomas H. Schindler, Johns Hopkins University, School of Medicine, Division of Nuclear Medicine, Cardiovascular Nuclear Medicine, Department of Radiology and Radiological Science SOM, JHOC 3225, 601 North Caroline Street, Baltimore, Maryland 21287. E-mail: tschind3@jhmi.edu.

PERSPECTIVES

COMPETENCY IN MEDICAL KNOWLEDGE: PET flow quantification is able to identify an impairment of coronary circulatory function in myocardial regions with sarcoid-induced inflammation, and this may reflect a mechanistic link between active-inflammatory cardiac sarcoid disease and cardiovascular outcome.

COMPETENCY IN PATIENT CARE AND PROCEDURAL SKILLS: Sequential application of PET assessment of myocardial inflammation and coronary circulatory dysfunction presents a unique tool to monitor and guide immune-suppressive treatment options in cardiac sarcoidosis patients and may lead to an improved clinical outcome pending further investigations.

TRANSLATIONAL OUTLOOK: Cardiac PET is applied to concurrently assess myocardial perfusion and inflammation for the identification of active-inflammatory cardiac sarcoidosis, which carries important diagnostic and prognostic information. Immune-suppressive treatment mediates not only a decrease in regional myocardial inflammation but also maintains global coronary vasodilator function. Conversely, ineffective immune-suppressive treatment results in unchanged or even increased regional inflammation and a worsening of global vasodilator capacity of the coronary circulation. Improvement of sarcoid-related coronary vasodilator dysfunction, as a potential target of treatment response apart from myocardial inflammation, may hold promise to further optimize and individualize medical care in the prevention of cardiomyopathy.

REFERENCES

1. Hamzeh N, Steckman DA, Sauer WH, Judson MA. Pathophysiology and clinical management of cardiac sarcoidosis. Nat Rev Cardiol 2015;12:278–88.

2. Silverman KJ, Hutchins GM, Bulkley BH. Cardiac sarcoid: a clinicopathologic study of 84 unselected patients with systemic sarcoidosis. Circulation 1978;58:1204–11.

3. Sharma OP, Maheshwari A, Thaker K. Myocardial sarcoidosis. Chest 1993;103:253–8.

4. Perry A, Vuitch F. Causes of death in patients with sarcoidosis: a morphologic study of 38 autopsies with clinicopathologic correlations. Arch Pathol Lab Med 1995;119:167–72.

5. Schatka I, Bengel FM. Advanced imaging of cardiac sarcoidosis. J Nucl Med 2014;55:99–106.

6. Schindler TH, Solnes LS. Role of PET/CT for the identification of cardiac sarcoid disease. Ann Nucl Cardiol 2015;1:79–86.

7. Mirsaeidi M, Machado RF, Schraufnagel D, Sweiss NJ, Baughman RP. Racial difference in sarcoidosis mortality in the United States. Chest 2015;147:438–49.

8. Blankstein R, Osborne M, Naya M, et al. Cardiac positron emission tomography enhances prognostic assessments of patients with suspected cardiac sarcoidosis. J Am Coll Cardiol 2014;63:329–36.

9. Youssef G, Leung E, Mylonas I, et al. The use of 18F-FDG PET in the diagnosis of cardiac sarcoidosis: a systematic review and metaanalysis including the Ontario experience. J Nucl Med 2012;53:241–8.

10. Gould KL, Pan T, Loghin C, Johnson NP, Guha A, Sdringola S. Frequent diagnostic errors in cardiac PET/CT due to misregistration of CT attenuation and emission PET images: a definitive analysis of causes, consequences, and corrections. J Nucl Med 2007;48:1112–21.

11. Valenta I, Quercioli A, Vincenti G, et al. Structural epicardial disease and microvascular function are determinants of an abnormal longitudinal myocardial blood flow difference in cardiovascular risk individuals as determined with PET/CT. J Nucl Cardiol 2010;17:1023–33.

12. Slomka PJ, Alexanderson E, Jacome R, et al. Comparison of clinical tools for measurements of regional stress and rest myocardial blood flow assessed with 13N-ammonia PET/CT. J Nucl Med 2012;53:171–81.

13. Iozzo P, Chareonthaitawee P, Di Terlizzi M, Betteridge DJ, Ferrannini E, Camici PG. Regional myocardial blood flow and glucose utilization during fasting and physiological hyperinsulinemia in humans. Am J Physiol Endocrinol Metab 2002;282:E1163–71.

14. Williams G, Kolodny GM. Suppression of myocardial 18F-FDG uptake by preparing patients with a high-fat, low-carbohydrate diet. Am J Roentgenol 2008;190:W151–6.

15. Osborne MT, Hulten EA, Singh A, et al. Reduction in ^{18}F-fluorodeoxyglucose uptake on serial cardiac positron emission tomography is associated with improved left ventricular ejection fraction in patients with cardiac sarcoidosis. J Nucl Cardiol 2014;21:166–74.

16. McArdle B, Dowsley TF, Cocker MS, et al. Cardiac PET: metabolic and functional imaging of the myocardium. Semin Nucl Med 2013;43:434–48.

17. Schindler TH, Zhang XL, Vincenti G, Mhiri L, Lerch R, Schelbert HR. Role of PET in the evaluation and understanding of coronary physiology. J Nucl Cardiol 2007;14:589–603.

18. Schindler TH, Dilsizian V. PET-determined hyperemic myocardial blood flow: further progress to clinical application. J Am Coll Cardiol 2014;64:1476–8.

19. Schindler TH, Schelbert HR, Quercioli A, Dilsizian V. Cardiac PET imaging for the detection and monitoring of coronary artery disease and microvascular health. J Am Coll Cardiol Img 2010;3:623–40.

20. Lim SL, Lam CS, Segers VF, Brutsaert DL, De Keulenaer GW. Cardiac endothelium-myocyte interaction: clinical opportunities for new heart failure therapies regardless of ejection fraction. Eur Heart J 2015;36:2050–60.

KEY WORDS blood flow, circulation, inflammation, microvascular function, myocardial flow reserve, myocardial perfusion, positron emission tomography, sarcoid disease